Spatial and temporal variability of ozone and nitrogen dioxide over a major urban estuarine ecosystem

Maria Tzortziou, Jay R. Herman, Alexander Cede, Christopher P. Loughner, Nader Abuhassan & Sheenali Naik

Journal of Atmospheric Chemistry

ISSN 0167-7764

J Atmos Chem
DOI 10.1007/s10874-013-9255-8

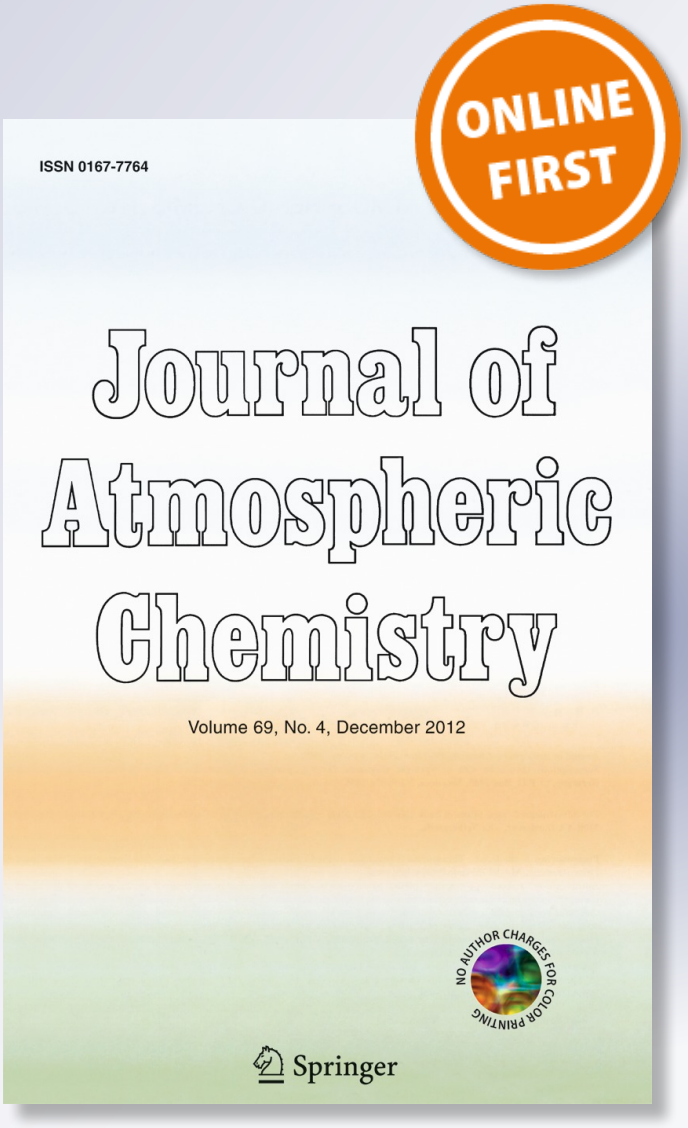

Springer

J Atmos Chem
DOI 10.1007/s10874-013-9255-8

Spatial and temporal variability of ozone and nitrogen dioxide over a major urban estuarine ecosystem

Maria Tzortziou · Jay R. Herman · Alexander Cede · Christopher P. Loughner · Nader Abuhassan · Sheenali Naik

Received: 2 January 2013 / Accepted: 22 March 2013

Abstract Spatial and temporal dynamics in trace gas pollutants were examined over a major urban estuarine ecosystem, using a new network of ground-based Pandora spectrometers deployed at strategic locations along the Washington-Baltimore corridor and the Chesapeake Bay. Total column ozone (TCO_3) and nitrogen dioxide ($TCNO_2$) were measured during NASA's DISCOVER-AQ and GeoCAPE-CBODAQ campaigns in July 2011. The Pandora network provided high-resolution information on air-quality variability, local pollution conditions, large-scale meteorological influences, and interdependencies of ozone and its major precursor, NO_2. Measurements were used to compare with air-quality model simulations (CMAQ), evaluate Aura-OMI satellite retrievals, and assess advantages and limitations of space-based observations under a range of conditions. During the campaign, $TCNO_2$ varied by an order of magnitude, both spatially and temporally. Although fairly constant in rural regions, $TCNO_2$ showed clear diurnal and weekly patterns in polluted urban areas caused by changes in near-surface emissions. With a coarse resolution and an overpass at around 13:30 local time, OMI cannot detect this strong variability in NO_2, missing pollution peaks from industrial and rush hour activities. Not as highly variable as NO_2, TCO_3 was mostly affected by large-scale meteorological patterns as observed by OMI. A clear weekly cycle in TCO_3, with minima over the weekend, was due to a combination of weekly weather patterns and changes in near-surface NO_x emissions. A Pandora instrument intercomparison under the same conditions

M. Tzortziou · C. P. Loughner
University of Maryland, Earth System Science Interdisciplinary Center, College Park, MD 20742, USA

M. Tzortziou (✉) · J. R. Herman · A. Cede · C. P. Loughner · N. Abuhassan
NASA/Goddard Space Flight Center, Greenbelt, MD 20771, USA
e-mail: maria.a.tzortziou@nasa.gov

J. R. Herman · N. Abuhassan
University of Maryland, Joint Center for Earth Systems Technology, Baltimore, MD 21228, USA

A. Cede
LuftBlick, Kreith, Austria

S. Naik
Environmental Science and Policy Department, University of Maryland, College Park, MD 20742, USA

Published online: 28 April 2013

at GSFC showed excellent agreement, within ±4.8DU for TCO_3 and ±0.07DU for $TCNO_2$ with no air-mass-factor dependence, suggesting that observed variability during the campaign was real.

Keywords Ozone · Nitrogen dioxide · Atmospheric variability · Urban · Coastal · Remote sensing

1 Introduction

Atmospheric composition has changed significantly over the past few decades from increasing urbanization and as a response to environmental policy changes (e.g. Wenig et al. 2003; Vingarzan 2004; Parrish et al. 2009). Among major anthropogenic pollutants, nitrogen oxides ($NO + NO_2 = NO_x$) play a key role in atmospheric chemistry, affecting air quality, photochemical processes, climate radiative forcing, and human health (Crutzen 1979, 1995; Seinfeld and Pandis 1998; EPA 1998; Solomon 1999; Velders et al. 2001; IPCC 2007). Acting as a main precursor to tropospheric ozone (O_3), NO_x has received major attention by regulators and policy makers in efforts to curtail the formation of ozone. High ground-level O_3 concentrations can be toxic upon inhalation or contact, causing moderate to large (well over 20 %) decreases in lung function, respiratory illness, and other health and environmental problems (OAQPS 1996; EPA 2002).

Influenced by both natural and anthropogenic emissions, large and highly variable tropospheric NO_2 amounts often interfere with satellite retrievals of atmospheric aerosol optical depth and absorption. Over coastal waters close to heavily polluted urban centers, NO_2 is a significant (although, until recently, largely ignored) component affecting the top-of-atmosphere (TOA) signal measured by an ocean color satellite sensor at wavelengths traditionally used for retrievals of chlorophyll-a and colored dissolved organic matter (O'Reilly et al. 2000; Carder et al. 1999; Ahmad et al. 2007; Mannino et al. 2008; Fishman et al. 2012; Tzortziou et al. 2012). Spatially and temporally varying O_3 concentrations also impact the accuracy of ocean color atmospheric corrections (Gordon 1997).

The environmental impacts of NO_2 and O_3 are not confined to the atmosphere. In highly polluted coastal urban areas, the atmosphere is a source of excess nutrients and pollutants to the land and coastal ocean, contributing to the degradation of terrestrial and aquatic ecosystem health. NO_2 can act as an acidifying and eutrophying agent in terrestrial and aquatic ecosystems through dry or wet deposition of its oxidation products (e.g. Jickells 2006). Close to urban areas, dry deposition of NO_x can be particularly important (Dennis 2007). Along the eastern US coast, deposition of atmospheric nitrogen has been shown to account for as much as 70 % of total nitrogen loadings to estuaries (Castro et al. 2003). In the Chesapeake Bay, the largest estuary in the US and one of the most productive in the world, at least one third, and probably significantly more, of total nitrogen inputs comes from air deposition (STAC Publ. 09-001 2009). Ozone deposition can damage plants and reduce crop yields (Booker et al. 2009; Fishman et al. 2010; Sanders et al. 1992). These atmospheric inputs increase pressure on coastal ecosystems already stressed by a wide range of other human activities (e.g., nitrogen bearing chemical runoff from land).

Measurements of NO_2 from both ground- and space-based instruments typically show strong temporal and spatial variability, reflecting the importance of urban areas as hot-spots of NO_x emissions and the influence of various NO_x sources on local and trans-boundary pollution episodes (Wenig et al. 2003; Beirle et al. 2004; Boersma et al. 2005; Choi et al. 2005; Herman et al. 2009). Satellite measurements with GOME-1 (Global Ozone

Monitoring Experiment) (Burrows et al. 1999), SCIAMACHY (SCanning Imaging Absorption spectroMeter for Atmospheric CHartographY) (Bovensmann et al. 1999), GOME-2 (Callies et al. 2000), and OMI (Ozone Monitoring Instrument) (e.g. Levelt et al. 2006; Celarier et al. 2008) have provided valuable information on the spatial variability in NO_2 and its seasonal and weekly patterns. Comparisons of measurements from different satellite instruments have revealed large differences between morning and afternoon total column NO_2 ($TCNO_2$) amounts, driven by emissions and photochemistry (e.g. Beirle et al. 2004; Richter et al. 2005; Boersma et al. 2008).

Although not as highly variable in space and time as NO_2, total column ozone (TCO_3) often shows significant spatiotemporal variability. Using both Aura-OMI satellite observations and high resolution ground-based measurements, Tzortziou et al. (2012) reported sharp spikes and dips in TCO_3, of the order of 20 DU within less than 2 h, associated mostly with highly dynamic weather systems such as pressure changes, passage of a cold front with high stratospheric ozone content, or intrusion of low-ozone air from lower latitudes. Considerable variability over the course of a day, on some days as high as 40 to 50 DU, was found in TCO_3 at several mid- to high-latitude sites in the US and Europe (Tzortziou et al. 2012).

Photochemical smog (NO_x and ozone pollution) remains a serious problem in many coastal cities worldwide, both in industrialized and, particularly, in developing economies where rapid coastal urbanization is presently occurring (e.g. Pineda Rojas and Venegas 2009; Gu et al. 2011). High resolution ground-based measurements of trace gases are essential in urban coastal areas to 1) better understand atmospheric dynamics at higher spatial resolution than is currently available from satellite observations, 2) capture the high temporal variability associated with local pollution patterns and photochemical processes, and 3) make measurements of atmospheric trace gases and pollutants relevant to our understanding of urban and coastal ecosystem dynamics. In this paper we present new, high-resolution, continuous measurements of total column O_3 and NO_2 spatial and temporal variability over the Washington DC/Baltimore metropolitan area and the Chesapeake Bay estuary, using a network of ground-based Pandora spectrometer systems. The small size and portability of the Pandora instruments allowed deployment at strategic locations within this major urban estuarine system for capturing short-term and small-scale dynamics in trace gas amounts and assessing influences of both regional near-surface pollution emissions and larger scale meteorological processes. Such information is critical for evaluating satellite trace-gas retrievals under a range of conditions. Measurements were performed during July 2011, as part of two simultaneous field campaigns in the region: the DISCOVER-AQ (Deriving Information on Surface Conditions from Column and Vertically-Resolved Observations Relevant to Air Quality) and the GeoCAPE-CBODAQ (Geostationary Coastal and Air Pollution Events-Chesapeake Bay Oceanographic Campaign with DISCOVER-AQ) field campaigns.

2 Methods

2.1 Study sites

The DISCOVER-AQ project is a four-year NASA Earth Venture mission to improve the use of satellites to monitor air quality for public health and environmental benefit. Through targeted airborne and ground-based observations, DISCOVER-AQ aims at improving the interpretation of satellite observations to diagnose near-surface conditions relating to air

quality. The first of four planned deployments took place over the Washington, DC and Baltimore, MD metropolitan area and the Chesapeake Bay shoreline throughout the month of July 2011. Two aircraft were used, the NASA P-3B for in-situ sampling in the lowest 3 km of the atmosphere and the NASA UC-12 flying at ~9 km with remote sensing instruments for trace gases and aerosols. In addition, extensive ground observations were used to measure air pollution at the surface using in-situ observations, and aloft, using balloons and remote sensing instruments. The GeoCAPE-CBODAQ field campaign complemented the DISCOVER-AQ campaign by making ship-based measurements of air and water quality from 11 to 20 July 2011. As part of these campaigns, a network of Pandora CCD and CMOS spectrometers provided continuous (every 20 s), high-resolution measurements of total column NO_2 and O_3 amounts at twelve urban and rural locations characterized by different levels of pollution (Fig. 1 and Table 1).

The Baltimore–Washington corridor experiences poor air quality throughout the year for particulate matter, while high ozone amounts tend to be limited to the April–September timeframe (Maryland Dept. of the Environment, Air Quality Seasonal Reports, 2008). Both pollutants historically peak in the June–August timeframe. Emissions associated with transportation, biogenic emissions, and transport of background pollution from upwind locations all play an important role in generating poor air quality over this region (http://discover-aq.larc.nasa.gov/pdf/DISCOVER-AQ_science.pdf). Meteorological processes along the Chesapeake Bay land-sea interface and mesoscale phenomena, such as bay breeze circulations, additionally impact transport and transformation of NO_x and O_3 over this region (Loughner et al. 2011; Loughner et al. 2013).

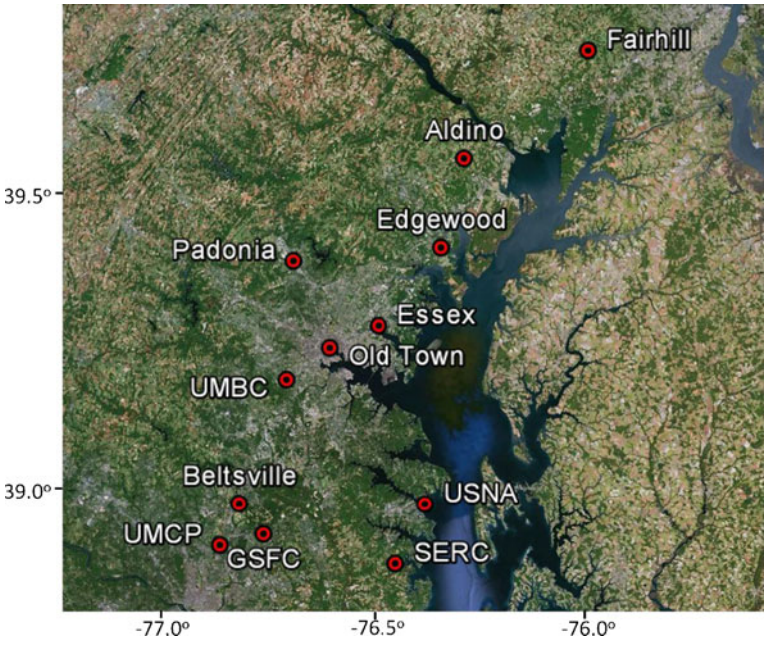

Fig. 1 Map of the network of Pandora spectrometers deployed during the DISCOVER-AQ and CBODAQ field campaigns in July 2011

Table 1 Pandora network sites and Pandora instrument used at each site, during the DISCOVER-AQ and CBODAQ NASA field campaigns in July 2011

Site	Latitude	Longitude	Pandora #
University of Maryland Baltimore County (UMBC)	39.252	−76.709	2 (CCD)
Goddard Space Flight Center (GSFC)	38.993	−76.839	3 (CCD)
Smithsonian Environmental Research Center (SERC)	38.889	−76.559	7 (CMOS)
Old Town	39.290	−76.596	9 (CMOS)
Fairhill	39.701	−75.860	16 (CCD)
Padonia	39.455	−76.633	17 (CCD)
Edgewood	39.419	−76.294	18 (CCD)
Essex	39.309	−76.475	19 (CCD)
Beltsville	39.055	−76.878	20 (CCD)
University of Maryland College Park (UMCP)	38.990	−76.942	21 (CCD)
Aldino	39.564	−76.196	23 (CCD)
United States Naval Academy	38.981	−76.4625	25 (CCD)

2.2 Pandora technical characteristics

A detailed description of the Pandora instrument technical characteristics is provided in Herman et al. (2009). Briefly, the Pandora spectrometer system consists of an optical head sensor, mounted on a computer controlled sun-tracker and sky-scanner (~0.01° pointing precision), and connected to an Avantes array spectrometer by means of a 400 micron core-diameter single strand multi-mode optical fiber. To achieve wavelength and radiometric calibration stability, the spectrometer is temperature stabilized inside an insulated enclosure using an actively coupled thermo-electric cooler and heater. There are two versions of the Pandora spectrometer system, the Sun-only CMOS detector Pandora (280–500 nm) and the CCD detector Sun-and-Sky Pandora (280–525 nm) (Table 1 in Tzortziou et al. 2012). The CMOS and CCD spectrometers have the same accuracy, with CMOS instruments having somewhat higher noise. All of the newer instruments are based on CCD detectors. Pandora has a spectral resolution of 0.6 nm and a field of view (FOV) of about 1.6° full width half maximum (FWHM).

The CMOS Pandora spectrometer system operates only in direct-sun observation, as it is not sensitive enough to measure sky radiances. The CCD version is about 10^3 times more sensitive (partly from the detector and partly from the addition of a lens to focus light on the optical fiber) and detects sky radiances easily. The CMOS Sun-only Pandora uses an Avantes spectrometer with a 1024 pixel detector, while the Sun-and-Sky Pandora uses an Avantes spectrometer with a UV sensitive back-thinned 2048 × 16 pixel or 2048 × 64 CCD. The open-hole and neutral density filters (ND1, ND2, ND3, and ND4) in the first filterwheel give a 10,000:1 dynamic range, which, combined with the exposure range 4–4000 ms, gives an overall dynamic range of 10^7 needed for sun and sky observations at all latitudes and in all seasons.

Wavelength calibration and slit functions for the Pandora instruments are determined from lamp emission lines (Hg, Cd, Cu, In, Mg, Zn). Wavelength stability is validated during field use by an analysis of the solar Fraunhofer line structures. Stray light is reduced for Pandora measurements in the 310 to 330 nm range using two UV band pass filters, BP300 (280–320 nm) and U340 (280–380 nm) with cutoffs at 320 and 380 nm, respectively. A

further stray light correction is obtained from pixels corresponding to 280 to 285 nm, which contain almost zero direct illumination. Previous comparisons between a well-calibrated double grating Brewer spectrometer (#171) characterized by a very low internal stray light fraction at the short UV-B wavelengths ($<10^{-7}$) and Pandora showed very good agreement up to slant column ozone amounts of 1,500 DU (or solar zenith angles, SZAs, up to 80°). The practically negligible SZA dependence of the TCO_3 residuals showed that the stray-light correction method applied to Pandora provides an adequate correction (Tzortziou et al. 2012).

2.3 Pandora total column ozone and NO_2 algorithm

Here we analyze TCO_3 and $TCNO_2$ amounts from both CMOS and CCD detector Pandora spectrometers operated in direct-sun viewing mode (Table 1). The spectral fitting algorithm uses laboratory measured absorption cross sections for each atmospheric absorber (i.e. O_3, NO_2, SO_2, HCHO, BrO for the 310–530 nm spectral region used here), a 4th order polynomial in wavelength to remove aerosols and Rayleigh scattering effects, and wavelength shift and squeeze functions to remove wavelength errors at the 1 picometer level. The shift and squeeze functions provide the best match to the measured spectrum compared to a solar reference spectrum containing the solar Fraunhofer line structure (Herman et al. 2009).

Pandora's direct-sun $TCNO_2$ includes both the troposphere (NO_2 amounts up to 2 DU or higher in urban areas) and a stratospheric contribution of 0.1 to 0.2 DU. The $TCNO_2$ retrieval uses laboratory NO_2 absorption cross sections (Vandaele et al. 1998), and laboratory calibration of Pandora (wavelength, slit function, and radiometric). The retrieval is done by spectral fitting over the range 400–440 nm. Absolute error in Pandora $TCNO_2$ retrievals is 0.1 DU, caused by an error in estimating residual stratospheric NO_2 amount by extrapolating to zero air mass using a modified Langley method (Herman et al. 2009; Wang et al. 2010). The CCD version has a precision of about 0.01 DU in clear skies from averaging about 4000 measurements in a 20 s interval, where the exposure time is adjusted to fill the CCD wells to about 80 %. The CMOS units have increased noise because the longer exposure time leads to fewer measurements averaged in 20 s. Similarly, in the presence of clouds the exposure time increases and the precision is reduced.

TCO_3 is determined using direct-sun measurements in the spectral range 310–330 nm and the high resolution O_3 cross sections from Daumont et al. (1992) at a nominal effective ozone temperature of T=225° K. Absolute TCO_3 retrievals are performed using the independently measured Kurucz (2005) ground-based extraterrestrial spectrum, radiometrically corrected to the Atlas-3 SUSIM spectrum (Van Hoosier, 1996) as described in Bernhard et al. (2004), and convoluted with the Pandora slit function to be used as a TOA reference spectrum (Tzortziou et al. 2012). This method is very different from the usual technique of using a TOA reference spectrum based on the instrument's own measurements from a Langley extrapolation to zero air mass (e.g. Herman et al. 2009). Using the independent spectrum technique gives an absolute TCO_3 measurement, since the reference spectrum is free of residual atmospheric absorption. It also avoids the errors associated with performing a Langley extrapolation (e.g., Gröbner and Kerr 2001; Bais 1997) of the Pandora measured solar spectrum to zero air-mass. While this method requires an accurate knowledge of the instrument's slit function as determined in the laboratory, it is insensitive to a radiometric calibration offset that only changes smoothly with wavelength. For example, a change that can be fit with a 4th order polynomial (Tzortziou et al. 2012).

2.4 OMI retrievals

The Ozone Monitoring Instrument (OMI), launched on NASA's Earth Observing System (EOS) AURA satellite on July 15, 2004, has been collecting data since August 9, 2004 (Levelt et al. 2006; Boersma et al. 2007). Aura flies in formation with the "A Train" satellite constellation, has a sun-synchronous polar orbit at approximately 705 km altitude with a period of 100 min and a local equator crossing time between 13:40 and 13:50 local time. OMI is a cross-track downward viewing near-UV/Visible CCD spectrometer that provides near-global coverage in one day. The size of an OMI pixel varies with cross-track viewing zenith angle from 24 km in the nadir to approximately 128 km for the extreme viewing angles of 57^{o} at the edges of the swath (Boersma et al. 2007). OMI measurements cover a spectral region of 264–504 nm with a spectral resolution between 0.42 nm and 0.63 nm, and provide retrievals of a number of trace gases including O_3, NO_2, SO_2, HCHO, BrO, and OClO. In addition, OMI measures aerosol characteristics, cloud top heights and cloud coverage, and can estimate UV irradiance at the Earth's surface (Levelt et al. 2006).

The EOS Aura OMI OMNO2-L2OVP (Data Set Version 003) NO_2 product is used in this study (http://avdc.gsfc.nasa.gov, Data Set Release date: July 2012). This product contains the slant Column NO_2 (total amount along the optical path from the sun into the atmosphere and then toward the satellite), the total vertical column NO_2, and the estimated tropospheric portion of the total column NO_2. Other ancillary data are also provided in the OMI OMNO2-L2OVP file, including data quality flags, measures of precision, and quality assurance information. The slant column amount NO_2 is determined from a spectral fit to the Earth reflectance spectrum using the Differential Optical Absorption Spectroscopy (DOAS) method (Platt 1994; Boersma et al. 2002; Bucsela et al. 2006). The fitting algorithm is applied in the spectral range 405–465 nm using the Vandaele et al. (1998) NO_2 absorption cross sections convoluted with the measured OMI slit function. Total vertical column NO_2 amounts are estimated from the measured slant column using computed air mass factors (AMFs) and a monthly mean climatology of NO_2 profile shapes constructed from the Global Modeling Initiative (GMI) Chemical Transport Model simulation (Palmer et al. 2001; Krotkov et al. 2012).

The OMI-TOMS OMTO3 V8.5 O_3 product is used for TCO_3 comparisons in this study (http://avdc.gsfc.nasa.gov). The OMI-TOMS TCO_3 algorithm uses four wavelengths (317.5 and 331.2 nm under most conditions, and 331.2 and 360 nm for high ozone and high solar zenith angle conditions), and is based on the NASATOMS V8 retrieval algorithm (Bhartia and Wellemeyer 2002). The retrieval applies corrections to remove errors caused mainly by aerosols, clouds, sea glint, and SO_2 absorption. TCO_3 data provided by the OMI-TOMS algorithm have a root-mean square error of 1–2 %, depending on solar zenith angle, aerosol amount, and cloud cover (OMTO3_V003 ReadMe file, Released April 3, 2012) .

Here, we compare Pandora results with OMI $TCNO_2$ and TCO_3 station overpass data (http://avdc.gsfc.nasa.gov/index.php?site=1593048672&id=28). OMI station overpass data files provide the nearest OMI measurement in an OMI track (orbit), if it is closer than 100 km, to the ground-station. Typically, one to two overpasses per day are available, and occasionally three overpasses separated by 100 min. Among other parameters, the data files contain information on the distance between the overpass location point and the OMI FOV, the OMI cross track position CTP (0-59), and the radiative cloud fraction.

3 Results and discussion

3.1 Ground-based instrument inter-comparison

The DISCOVER-AQ deployment of a network of twelve Pandora spectrometers at strategic locations within the campaign study region provided information not only on the temporal, but also on the spatial variability in $TCNO_2$ and TCO_3 amounts. This information is key for understanding the local effects of anthropogenic activities (automobiles, power plants, etc.), regional conditions, and large-scale meteorological phenomena on atmospheric composition. It is also needed for integrating with coarser resolution satellite observations, and evaluating high-resolution model predictions of atmospheric chemistry and tropospheric air quality.

To use the measurements from a network of different Pandora spectrometers to address questions relevant to spatial patterns in atmospheric trace gases, an instrument inter-comparison is essential to determine instrument performance characteristics under the same conditions and detect any consistent instrument offsets. Such an instrument inter-comparison was performed at the GSFC site at the end of the July campaign using all Pandora

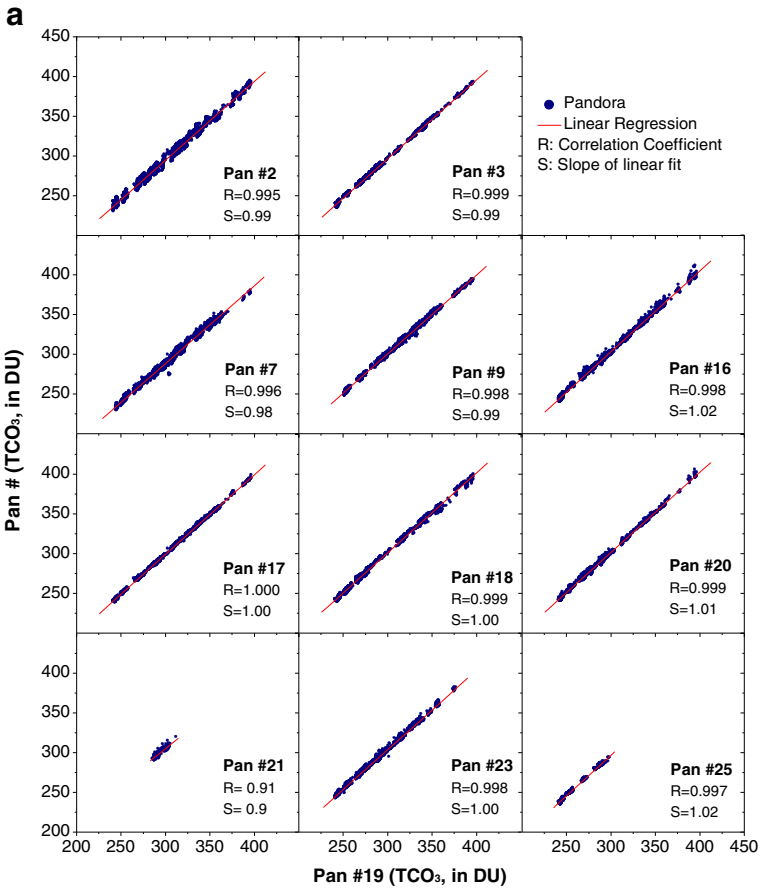

Fig. 2 Instrument intercomparison results at GSFC for (**a**) TCO_3 and (**b**) $TCNO_2$

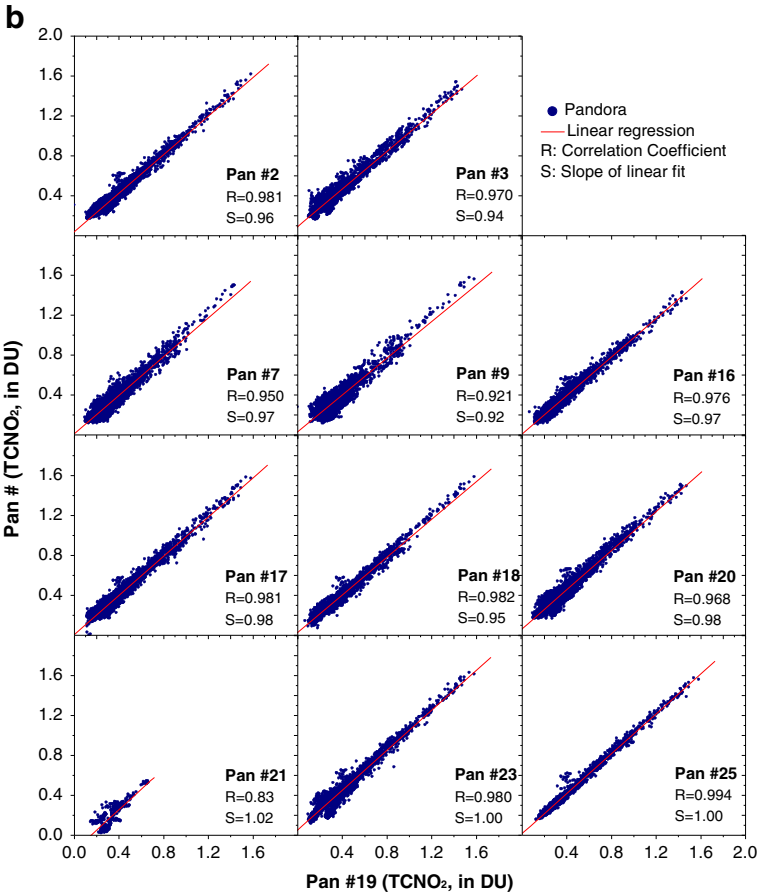

Fig. 2 (continued)

spectrometers deployed during DISCOVER-AQ (Table 1). Intercomparison measurements covered the period from October 2011 to February 2012, except for Pandora #21, which was at GSFC for only a few days in August, as it was deployed to Helsinki, Finland, in September 2011 (Tzortziou et al. 2012). Pandora #19 was selected as a reference data set for the purposes of displaying the data in Figs. 2 and 3. In addition, measurements from Pandora #21 were compared to Pandora #3, because it was the only other instrument operating at GSFC during August 2011. For consistency, results for #21 are shown in Figs. 2 and 3 relative to Pandora #19, based on the comparison between Pandoras #19 and #3.

Pandora data were filtered for normalized root-mean square of weighted spectral fitting residuals (nRMS) less than 0.05, uncertainty in NO_2 retrievals less than 0.05 DU, uncertainty in O_3 retrievals less than 2 DU, solar zenith angle (SZA) less than 70°, and retrieved wavelength shift less than 0.01 nm. In addition, for the CCD instruments (all but CMOS instruments #7 and #9) we only used measurements with filter-wheel positions 3 or 4 for cloud screening.

Excellent agreement in TCO_3 retrievals was found among the different Pandoras during the inter-comparison at GSFC (Figs. 2a, 3a). Linear regression between each Pandora and

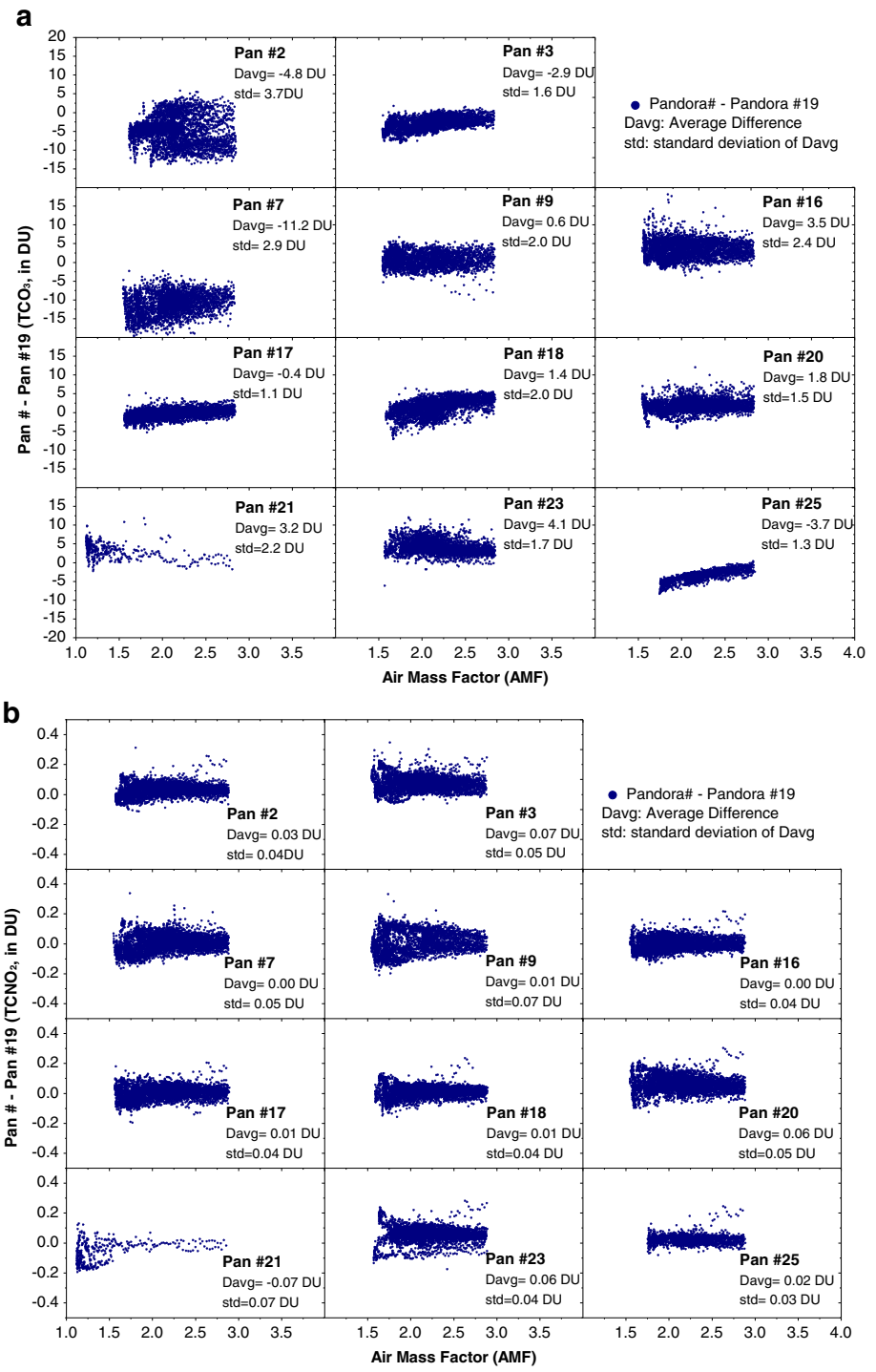

Fig. 3 **a** Difference in TCO_3 between each Pandora instrument and the reference (Pandora #19), as a function of air mass factor (AMF). **b** Same as in (**a**), for $TCNO_2$

the reference instrument resulted in strong correlations (in almost all cases correlation coefficient, R, was better than 0.995) and slopes ranging between 0.98 and 1.02 (Fig. 2a). Average differences (D_{avg}) in TCO_3 were in all cases within ±4.8 DU, or ±1.5 %, except for Pandora #7 (Fig. 3a). This instrument, located at SERC during the campaign, was the only instrument that had a consistent negative bias during the intercomparison at GSFC, underestimating TCO_3 on average by 11.2 DU, or 4 %, compared to the other Pandoras. To correct for this instrumental bias, SERC TCO_3 measurements by Pandora #7 were adjusted by +4 %. Differences between Pandora spectrometers during the intercomparison at GSFC showed almost no dependence on air mass factor (Fig. 3a).

Very good agreement was also found in $TCNO_2$ retrievals among Pandora instruments during the inter-comparison at GSFC (Figs. 2b, 3b). Linear regression between each Pandora and the reference resulted in strong correlations (although NO_2 results showed more scattering compared to TCO_3 retrievals) with slopes ranging between 0.92 and 1.2 (Fig. 2b). Absolute average differences in $TCNO_2$ were in all cases less than 0.07 DU, or 20 %, with more Pandoras showing average differences less than 0.02 DU, or 5 %. Pandora #7 did not show any significant bias in $TCNO_2$ retrievals compared to the other Pandoras (D_{avg} of just 0.004 DU compared to #19, Fig. 3b). Similar to results for TCO_3, differences in $TCNO_2$ between Pandora spectrometers showed almost no dependence on air mass factor (Fig. 3b).

3.2 Comparison between Pandora and Aura OMI

To enhance the scientific return of satellite remote sensing and obtain a more complete picture of the atmosphere, satellite observations should be combined with wide-area, high spatial and temporal resolution ground-based observations. This is necessary not only for satellite validation and evaluation of assumptions used in satellite retrievals, but also to better understand atmospheric dynamics at a higher spatial resolution than is currently available from satellite observations, and to capture the high temporal (e.g. hourly) variability in atmospheric pollutants such as nitrogen oxides associated with local emissions and photochemical processes.

Ground-based observations of $TCNO_2$ and TCO_3 amounts from Pandora were compared with space-based observations from Aura-OMI, to assess the degree of agreement between these two different remote sensing methods over the Washington DC-Chesapeake Bay urban estuarine environment (Figs. 4 and 5). For comparisons with satellite observations, Pandora TCO_3 data were averaged over a ±1-hr window around the OMI overpass time (Tzortziou et al. 2012). Due to the higher temporal variability typically observed in NO_2 relative to O_3, Pandora $TCNO_2$ data were averaged over a ±0.5-hr window around the OMI overpass time. Ground-based measurements were filtered to only include data with uncertainty in TCO_3 <2 DU, uncertainty in $TCNO_2$ <0.05 DU and normalized RMS of weighted spectral fitting residuals <0.05. OMI data were filtered to keep only those data where the OMI radiative cloud-fraction was <0.2 (Tzortziou et al. 2012; Reed et al. *this issue*). No filtering was applied for the OMI Cross Track Position (CTP) or the distance between the Pandora location and the OMI CTP, since there was little dependence on these parameters.

Good overall agreement was found between Pandora and OMI retrievals of TCO_3 in the study region (Fig. 4, Table 2), consistent with previous studies over a range of mid- to high-latitude sites in Europe and the US (Tzortziou et al. 2012). Average TCO_3 differences between ground-based and satellite data at the different sites were in all cases less than 12 DU, or 3.9 % (s.d. < 3.2 %), other than USNA where very limited data were available (N=8)

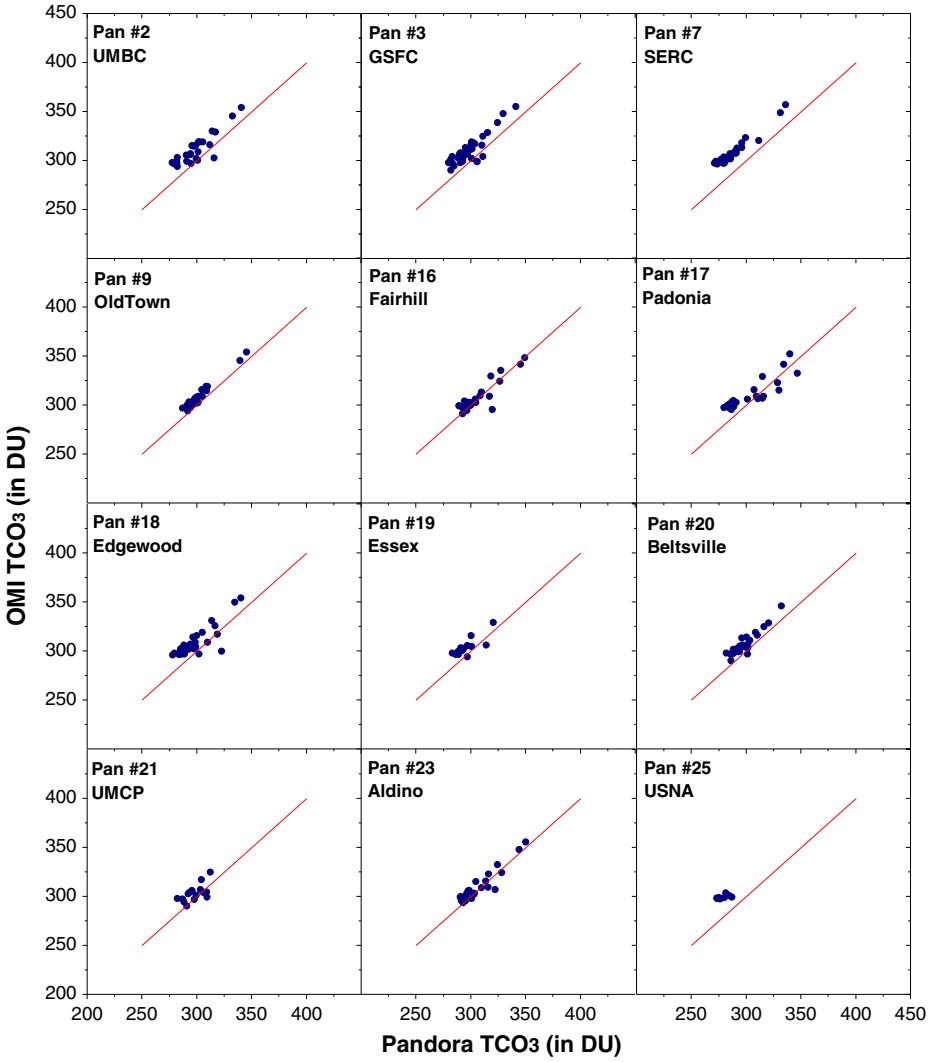

Fig. 4 OMI and Pandora TCO_3 retrievals (*circles*) at the different sites of the Pandora network during the campaign. The 1:1 line is also shown here (*red line*). Average differences, standard deviation and correlation coefficients between the two datasets are shown in Table 2

because Pandora was deployed at this location only after July 15th. Overall, Pandora slightly underestimated TCO_3 relative to OMI. The strongest correlation and best agreement between satellite and ground-based observations were found at SERC (R=0.97, D_{avg} =2.8 %), Fairhill (R=0.9, D_{avg}=0.3 %), Old Town (R=0.98, D_{avg}=1.6 %), and Beltsville (R=0.93, D_{avg}= 2.7 %), sites that range from rural to highly urban (Fig. 1).

Average differences between Pandora and OMI $TCNO_2$ retrievals ranged between -0.17 DU and 0.05 DU at the different sites (Fig. 5, Table 3). In most of the cases OMI underestimated $TCNO_2$. Particularly at GSFC, Old Town, Beltsville and UMCP, among the most polluted urban sites in the study region, OMI did not detect the high $TCNO_2$ amounts (0.4–1.0 DU) observed locally by the Pandora spectrometers (Fig. 5). Such regional

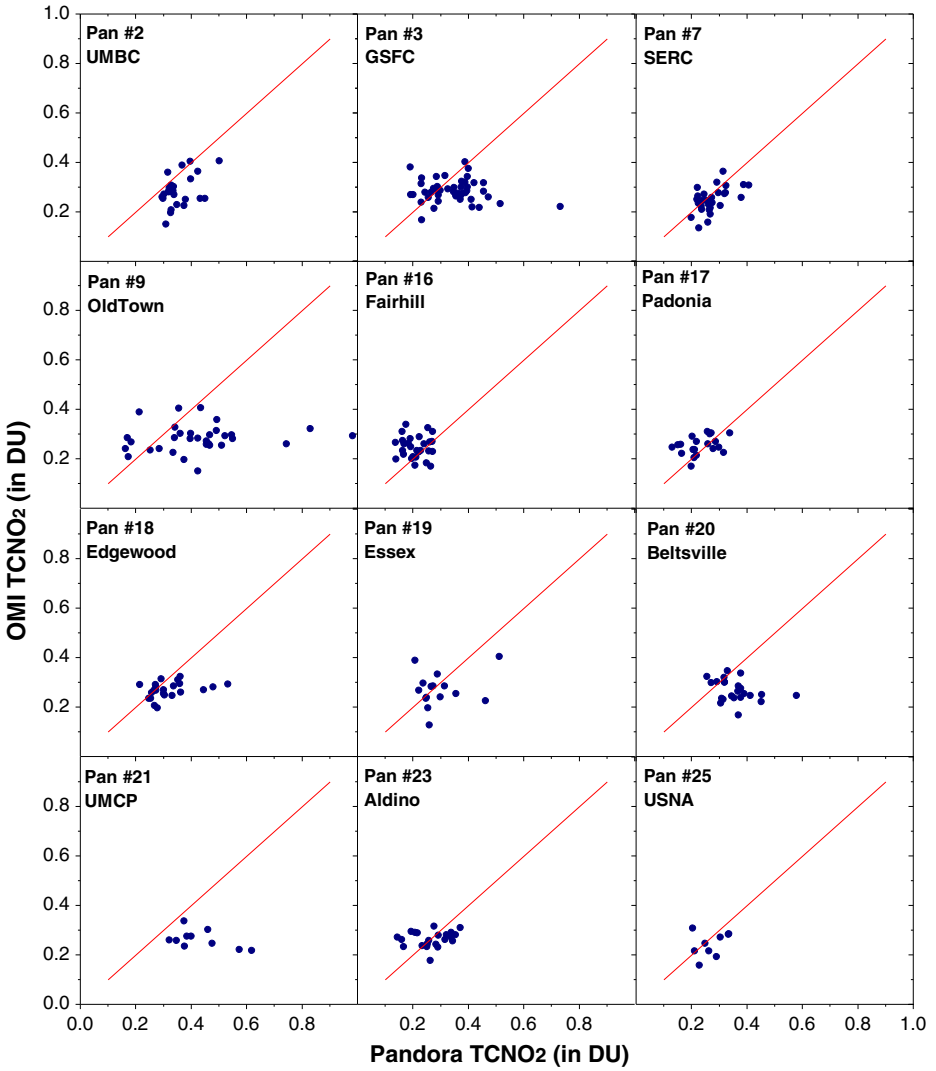

Fig. 5 OMI and Pandora $TCNO_2$ retrievals (*circles*) at the different sites of the Pandora network during the campaign. The 1:1 line is also shown here (*red line*). Average differences, standard deviation and correlation coefficients between the two datasets are shown in Table 3

peaks in $TCNO_2$ are typically associated with ground-level changes caused by local pollution. Correlation between satellite and ground-based retrievals was significantly worse for $TCNO_2$ compared to TCO_3 measurements (Table 3). This highlights the considerably stronger heterogeneity characterizing mostly tropospheric $TCNO_2$ fields, relative to mostly stratospheric TCO_3 amounts.

3.3 Spatial patterns and temporal dynamics in O_3 and NO_2

TCO_3 was fairly homogeneous spatially in the Washington-Baltimore region during July 2011. Differences among the TCO_3 values measured by the Pandora network on any given

Table 2 Average differences (D_{avg}) in TCO_3, shown in DU and in %, along with standard deviation (std), correlation coefficients (R), and number of coincident measurements (N) between OMI overpass and Pandora retrievals (OMI-Pandora) at the different sites of the Pandora network during the campaign

Site	Pan #	TCO_3 D_{avg} (±std)	TCO_3 $\%D_{avg}$ (±std)	R	N
UMBC	2	12 (±7)	3.9 (±2.5)	0.88	28
GSFC	3	12 (±7)	3.8 (±2.2)	0.88	36
SERC	7	9 (±4)	2.8 (±1.4)	0.97	26
Old Town	9	5 (±3)	1.6 (±1.1)	0.98	31
Fairhill	16	1 (±7)	0.3 (±2.3)	0.90	26
Padonia	17	7 (±10)	2.2 (±3.2)	0.89	27
Edgewood	18	10 (±9)	3.2 (±2.9)	0.84	29
Essex	19	8 (±6)	2.5 (±1.9)	0.80	17
Beltsville	20	8 (±4)	2.7 (±1.5)	0.93	27
UMCP	21	5 (±7)	1.7 (±2.4)	0.64	16
Aldino	23	2 (±6)	0.8 (±1.9)	0.93	26
USNA	25	20 (±5)	6.9 (±1.6)	0.52	8

day were of the order of ± 10 DU (Fig. 6), or ±3 %. At least half of this difference was due to real spatial variability in TCO_3, based on the results of the instrument intercomparison at GSFC showing agreement within ± 4.8 DU. The magnitude of this variability over the study region is consistent with the magnitude of average daily temporal variability observed at each individual site. Although temporal ozone changes as large as 30–35 DU were observed over the course of the day in certain cases, the average daily range in TCO_3 over the month of July ranged between 10 and 25 DU at the different Pandora sites. These results are consistent with previous studies on TCO_3 temporal variability measured by Pandora instruments at various mid- to high-latitude sites in Europe and the US (Tzortziou et al. 2012).

A large decrease in TCO_3 was observed over the whole Washington DC - Chesapeake Bay region at the beginning of July, with ozone dropping from approximately 350 DU on the morning of July 1st to 300 DU on July 3rd (Fig. 6). As shown in OMI satellite imagery, this

Table 3 Same as Table 2, for $TCNO_2$

Site	Pan #	$TCNO_2$ D_{avg} (±std)	$TCNO_2$ $\%D_{avg}$ (±std)	R	N
UMBC	2	−0.07 (±0.06)	−21.9 (±19.6)	0.44	25
GSFC	3	−0.06 (±0.11)	−19.7 (±36.2)	0.12	36
SERC	7	−0.03 (±0.05)	−10.7 (±19.0)	0.54	27
Old Town	9	−0.14 (±0.18)	−40.4 (±51.7)	0.13	30
Fairhill	16	0.04 (±0.06)	15.7 (±27.4)	−0.04	28
Padonia	17	0.02 (±0.06)	8.3 (±23.1)	0.36	20
Edgewood	18	−0.05 (±0.07)	−17.7 (±25.0)	0.34	23
Essex	19	−0.03 (±0.10)	−9.1 (±34.2)	0.23	15
Beltsville	20	−0.09 (±0.09)	−29.5 (±30.1)	−0.34	23
UMCP	21	−0.17 (±0.12)	−49.2 (±35.1)	−0.51	10
Aldino	23	0.00 (±0.07)	−1.2 (±24.8)	0.19	23
USNA	25	−0.03 (±0.06)	−10.7 (±22.9)	0.31	9

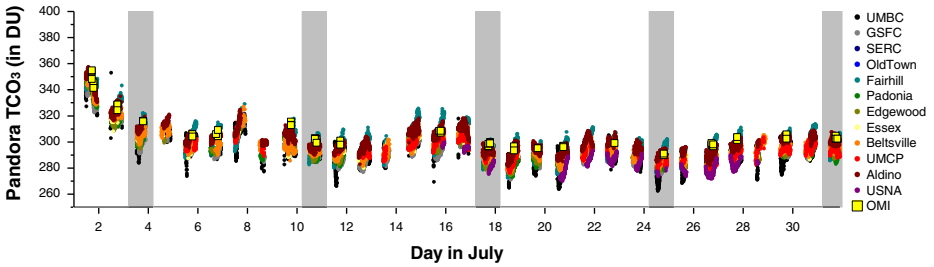

Fig. 6 Observed spatial and temporal variability in TCO_3 (in DU) as observed by the Pandora network (*circles*) during the campaign. Different Pandora sites are shown with different color. OMI overpass data for Fairhill, UMBC and Beltsville is also shown (*squares*). Measurements during Sundays (3, 10, 17, 24 and 31 July 2011) are indicated by the shaded area

sharp change in TCO_3 was due to the passage of a front transporting air masses with total column ozone amount of 350–375 DU over the campaign region during June 29th to July 1st (Fig. 7). Consistent with Pandora observations, OMI TCO_3 over the region dropped to 300–325 DU on July 3rd and July 4th. Pandora TCO_3 did not show large temporal variability from day to day during the rest of the campaign, with values remaining in the range of 290–310 DU. Interestingly, a clear weekly TCO_3 pattern of approximately 10 DU was observed at most Pandora sites, with a minimum consistently observed on Sundays (Fig. 6). The Sunday minimum could be due to chance weekly weather patterns affecting mainly upper tropospheric and stratospheric ozone amounts, as this weekly pattern was observed across the whole region, at both rural and urban sites, and it was also detected to a certain degree by

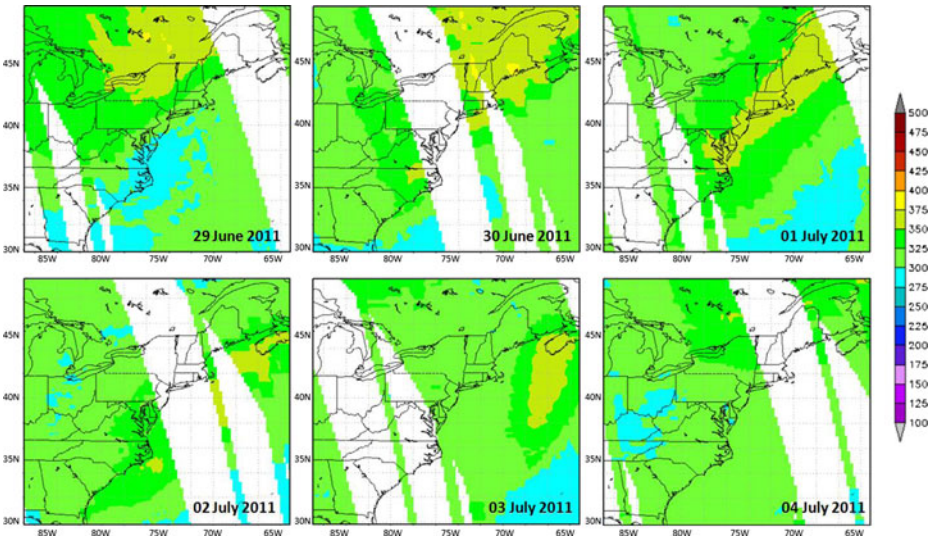

Fig. 7 Aura-OMI TCO_3 (DU) over the Eastern U.S. during June 29th and July 4th, 2011.The OMI images reveal the passage of a front moving from North to South and transporting air masses with higher TCO_3, in the range of 350 to 375 DU, over the Washington DC - Chesapeake Bay area on June 30th and July 1st. On July 2nd, TCO_3 over the area dropped to 325–350 DU, decreasing to 300–325 DU on July 3rd and July 4th. These OMI TCO_3 maps (OMI/Aura TOMS-like ozone product) were produced with the Giovanni online data system, developed and maintained by the NASA GES DISC

OMI (square symbols in Fig. 6). Air-quality model analysis and observed variability in NO_2, discussed in detail below, suggest that decreases in ground-level ozone amounts due to lower NO_x emissions over the weekend could also be partly responsible for the observed weekly pattern in TCO_3.

$TCNO_2$ varied by an order of magnitude, from 0.1 to 1 DU, both spatially over the study region and temporally (Figs. 5 and 8). The magnitude of this variability is significantly larger than the range of differences in $TCNO_2$ observed by the different Pandoras during the inter-comparison at GSFC ($|D_{avg}| < 0.07$ DU, std <0.07 DU; Fig. 3b), suggesting that the spatial NO_2 patterns observed during the campaign were real. According to the Pandora measurements, NO_2 at the more rural sites of the Pandora network (i.e. SERC, Fairhill and Padonia) was typically less than 0.4 DU and did not show significant temporal variability (Fig. 8a). In areas closer to highly polluted urban centers (i.e. GSFC, Beltsville and UMCP off the Washington-DC beltway, and Old Town and UMBC near Baltimore), $TCNO_2$ reached values as high as 1 DU (Fig. 8c). Although OMI was consistent with Pandora at low $TCNO_2$ amounts, it failed to detect $TCNO_2$ values higher than 0.4 DU often observed by Pandora during the satellite overpass time in areas characterized by higher pollution (Fig. 5).

At the urban sites, $TCNO_2$ showed a weekly cycle, with minimum values consistently observed over the weekend and maxima observed in the middle of the week (Fig. 8c). Such a behavior in $TCNO_2$ with respect to day of the week has been previously reported for the GSFC site, based on Pandora measurements over a period of more than 2 years (October 2006 to December 2008) (Herman et al. 2009). What our new measurements revealed is that there was a well defined weekly pattern in $TCNO_2$ at the urban sites during the DISCOVER-AQ

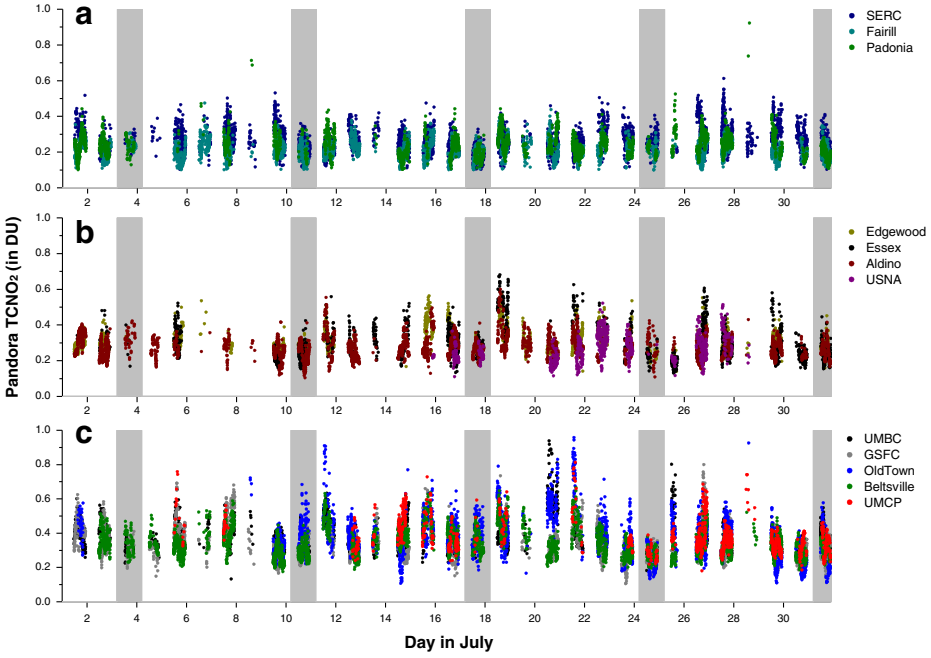

Fig. 8 Spatial and temporal variability in $TCNO_2$ (in DU) as observed by the Pandora network during the campaign. Different Pandora sites are shown with different color. Sites are grouped from rural (*upper panel*) to suburban (*mid panel*) and urban (*lower panel*). Measurements during Sundays (3, 10, 17, 24 and 31 July 2011) are indicated by the shaded area

campaign. The weekly pattern was significantly reduced at suburban sites typically characterized by lower traffic, Edgewood, Essex, Aldino and USNA (Fig. 8b), and it was absent in the relatively rural areas of SERC, Fairhill and Padonia (Fig. 8a).

Diurnal patterns in $TCNO_2$ were highly variable among stations, and also dependent on the day of the week (Fig. 9). In rural areas, $TCNO_2$ typically varied by less than a factor of 2 at each site without showing any consistent diurnal patterns. At the urban sites, though, and particularly at GSFC, Beltsville and Old Town, strong diurnal patterns were observed on most weekdays, with maxima in $TCNO_2$ typically occurring early in the morning and a second peak often observed later in the afternoon associated with rush-hour emissions. Peak $TCNO_2$ often reached 1 DU, five to ten times higher than background levels. A typical case is shown in Fig. 9 (blue solid circles), for Thursday July 21st. Observed diurnal patterns in NO_2 were considerably different over the weekend (Fig. 9, red open squares), when $TCNO_2$ amounts remained below 0.5 DU at both urban and rural sites, with no strong diurnal variability observed.

An analysis of $TCNO_2$ diurnal and day of the week dependence from an air quality model simulation agrees with the Pandora analysis (Fig. 10). The Environmental Protection Agency's (EPA) Community Multiscale Air Quality (CMAQ; Byun and Schere 2006) was run with a horizontal resolution down to 1.33 km for the entire DISCOVER-AQ field campaign. The CMAQ simulations were driven by meteorological fields from a Weather Research and Forecasting (WRF; Skamarock et al. 2008) model and included anthropogenic, biogenic, and lightning emissions (Loughner et al. 2013). Surface to 250 hPa NO_2 columns, averaged by day of the week from July 4 to July 31 during morning rush-hour conditions (1400–1500 UTC), reveal peak NO_2 values over urban areas on weekdays and the lowest values on weekends (Fig. 10a). During the OMI overpass time (1800–1900 UTC), however, lower NO_2 is predicted by CMAQ over the whole region and

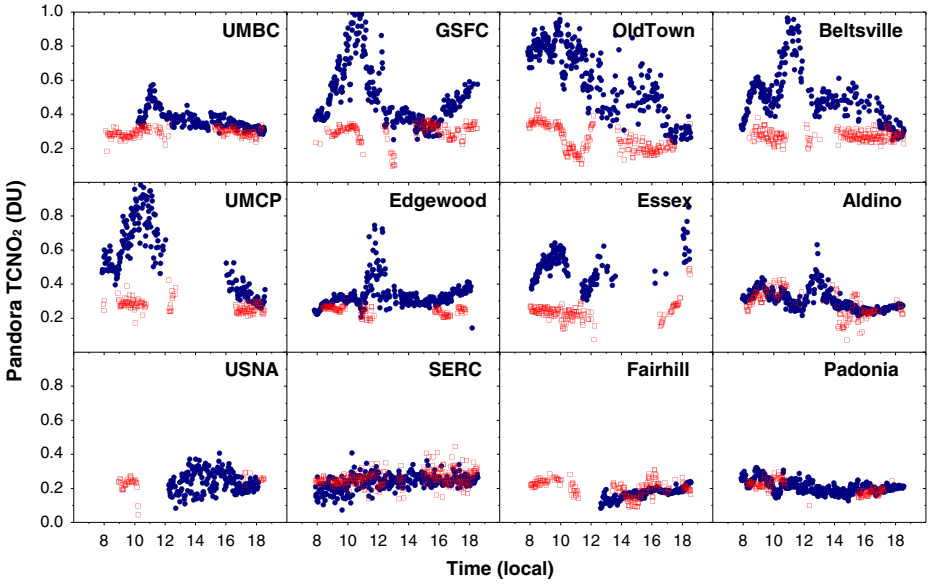

Fig. 9 Observed spatial and temporal variability in $TCNO_2$ (in DU) as observed by the Pandora network on Thursday 21 July 2011 (*blue solid circles*) and on Sunday 24 July 2011 (*open red squares*). Results highlight the strong spatial variability in $TCNO_2$ and differences in diurnal behavior with respect to day of the week

the weekly behavior and spatial heterogeneity in NO_2 are considerably reduced (Fig. 10b), consistent with Pandora observations.

A similar model analysis was performed for tropospheric ozone, to get some insights into the weekly cycle in TCO_3 observed by Pandora with minima on Sundays. Tropospheric O_3 formation is dependent on air pollution emissions and meteorology. To isolate the role of the day of the week dependence of emissions on tropospheric O_3 column, the CMAQ model was re-run for the weekend of 16–17 July 2011 using emissions appropriate for Wednesday, 13 July. Changing the emissions had little impact on model calculated O_3 column for Saturday, with the weekday emissions model run simulating surface to 500 hPa O_3 column at 1800 UTC to range from 0.7 DU lower to 0.9 DU higher than the weekend emissions model run. However, significant differences between the two CMAQ runs (weekday versus weekend emissions) were obtained for Sunday. The model

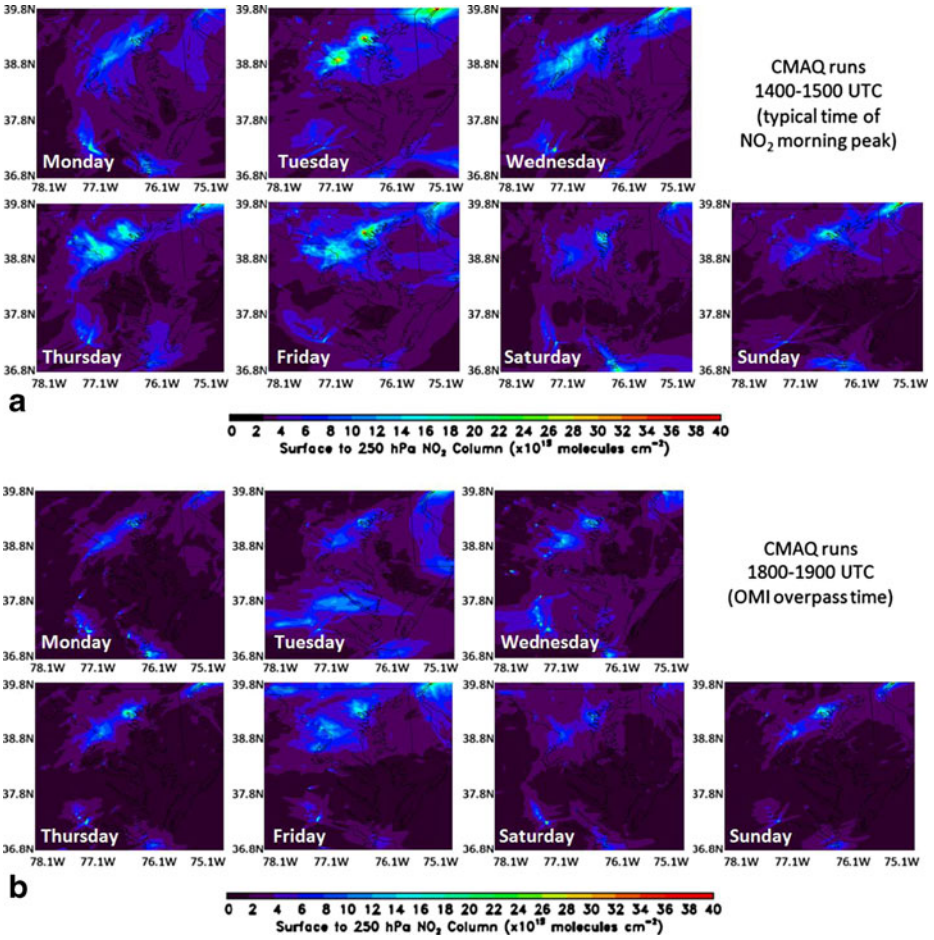

Fig. 10 Weekly behavior in NO_2 (surface to 250 hPa) as predicted by CMAQ. Daily averages during 4–31 July 2011 are shown here for: (**a**) 1400–1500 UTC, when maximum values in $TCNO_2$ typically occur at highly polluted urban sites, associated with morning rush-hour emissions; and (**b**) 1800–1900 UTC, during OMI overpass time, when spatial and day-to-day variability in $TCNO_2$ are considerably reduced

run with weekday emissions simulated higher surface to 500 hPa O_3 columns for Sunday at 1800 UTC, with maximum differences up to 1.9 DU in Baltimore, MD (Fig. 11). The weekday/weekend effect of emissions changes on tropospheric O_3 was evident in the model simulations for Sunday due to adequate time being elapsed since Friday allowing 1) air pollution differences from local emissions to buildup throughout the weekend due to

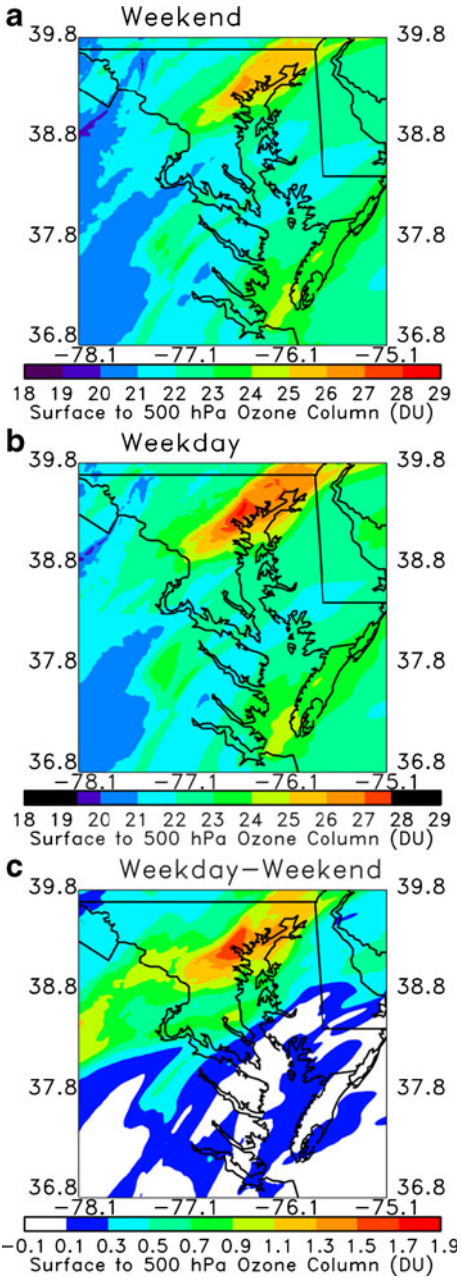

Fig. 11 CMAQ simulated surface to 500 hPa ozone column on Sunday, 17 July 2011 at 1800–1900 UTC using: (**a**) emissions appropriate for each day of the week (i.e., Sunday emissions), and (**b**) emissions appropriate for Wednesday, 13 July 2011. Differences between the two CMAQ runs are shown in **c**), and illustrate the weekday/weekend effect of emissions changes on tropospheric O_3

stagnation and 2) differences in air pollution emissions emitted 1 day upwind to be present over the Washington-Baltimore urban corridor.

4 Summary

Coastal areas close to heavily polluted urban centers are typically characterized by strong variability in atmospheric composition of trace gases. Continuous, high-resolution and high-precision measurements from a new network of twelve Pandora spectrometers deployed at strategic locations in the Washington DC- Chesapeake Bay region during the DISCOVER-AQ and CBODAQ field campaigns, captured the spatial and temporal dynamics in atmospheric O_3 and NO_2 over this major urban estuarine ecosystem. Measurements revealed strong spatial gradients and temporal patterns in trace gas amounts associated with human activities and local near-surface emissions of pollutants, larger scale meteorological influences, and interdependencies of ozone and its major precursor, NO_2.

Captured by both Pandora and satellite OMI observations, sharp gradients in TCO_3 by 50 DU at the beginning of the campaign were due to large scale meteorological processes transporting air masses with higher ozone content over the northeastern US coast. A clear weekly cycle in TCO_3 of about 10 DU and minimum values on Sundays were most likely due to weekly weather systems affecting mainly upper tropospheric and stratospheric ozone amounts. Decreases in ground-level ozone due to lower NO_x emissions over the weekend could also be partly responsible for the observed weekly pattern in TCO_3. A modeling sensitivity experiment isolating the impact of weekday/weekend emissions from the variability of the weather for one weekend in July revealed that a change in emissions from weekday to weekend caused surface to 500 hPa O_3 column to decrease up to ~2 DU. Although quite constant at rural sites, and typically less than 0.4 DU, $TCNO_2$ varied by as much as an order of magnitude in areas closer to highly polluted urban centers. In these regions, $TCNO_2$ showed a well defined weekly behavior and strong diurnal patterns associated with human activities and rush-hour peaks in near-surface NO_x emissions. These observed patterns in NO_2 were consistent with high-resolution air-quality model simulations using CMAQ.

With a footprint of approximately 12 km × 24 km at nadir and less sensitive to NO_2 concentrations near the surface where NO_x is emitted, OMI does not typically capture the strong spatial and temporal variability in NO_2 observed by the Pandora network and predicted by CMAQ. On a sun-synchronous polar orbit and with an overpass at around 13:30 local time, OMI misses the morning and late afternoon rush-hour peaks in $TCNO_2$ observed over urban areas on most weekdays, providing a satellite image of $TCNO_2$ under relatively low near-surface emission conditions. The results suggest that high resolution, long-term measurements from a network of ground based Pandora spectrometers can provide key information for improving understanding of atmospheric composition and dynamics over urban estuarine ecosystems, evaluating photochemical air-quality models, enhancing predictive modeling capabilities and assessing how future changes and management practices will affect ozone and its major precursors, climate, and air quality.

Acknowledgments This work was supported under the National Aeronautics and Space Administration (NASA) DISCOVER-AQ project (Grant: NNX10AR39G) and the NASA CBODAQ field campaign, with additional support from grants NASA.NNX10AQ79G and NASA.NNX11AP07G. The authors would like to thank Christian Retscher, James H. Crawford, Kenneth E. Pickering, Antonio Mannino, and two anonymous reviewers for their constructive comments and suggestions for improvement of the manuscript.

References

Ahmad, Z., McClain, C.R., Herman, J.R., Franz, B., Kwiatkowska, E., Robinson, W., Bucsela, E.J., Tzortziou, M.: Atmospheric correction for NO_2 absorption in retrieving water-leaving reflectances from the SeaWiFS and MODIS measurements". Appl. Opt. Laser Photonics Environ. Opt. **46**(26), 6504–6512 (2007)

Bais, A.F.: Absolute spectral measurements of direct solar ultraviolet irradiance with a Brewer spectrophotometer. Appl. Opt. **36**, 5199–5204 (1997)

Beirle, S., Platt, U., von Glasow, R., Wenig, M., Wagner, T.: Estimate of nitrogen oxide emissions from shipping by satellite remote sensing. Geophys. Res. Lett. **31**, (2004). doi:10.1029/2004GL020312

Bernhard, G., Booth, C.R., Ehramjian, J.C.: Version 2 data of the National Science Foundation's Ultraviolet Radiation Monitoring Network: South Pole. J. Geophys. Res. **109**, D21207 (2004). doi:10.1029/2004JD004937

Bhartia, P.K., Wellemeyer, C.W.: OMI TOMS-V8 Total O3 Algorithm, Algorithm Theoretical Baseline Document: OMI Ozone Products. P. K. Bhartia (ed.), vol. II, ATBD-OMI-02, version 2.0 (2002)

Boersma, K.F., Bucsela, E., Brinksma, E., Gleason, J.F.: NO2, Algorithm Theoretical Baseline Document: OMI Trace Gas Algorithms, K.Chance (ed.), vol. IV, ATBD-OMI-04, version 2.0 (2002)

Boersma, K.F., Eskes, H.J., Meijer, E.W., Kelder, H.M.: Estimates of lightning NO_x production from GOME satellite observations. Atmos. Phys. Chem. **5**, 2311–2331 (2005)

Boersma, K.F., Eskes, H.J., Veefkind, J.P., Brinksma, E.J., van der A, R.J., Sneep, M., van den Oord, G.H.J., Levelt, P.F., Stammes, P., Gleason, J.F., Bucsela, E.J.: Near-real time retrieval of tropospheric NO2 from OMI. Atmos. Chem. Phys. **7**(8), 2103–2118 (2007)

Boersma, K.F., Jacob, D.J., Eskes, H.J., Pinder, R.W., Wang, J., van der A, R.J.: Inter-comparison of SCIAMACHY and OMI tropospheric NO2 columns: observing the diurnal evolution of chemistry and emissions from space. J. Geophys. Res. **113**, (2008). doi:10.1029/2007JD008816

Booker, F., Muntifering, R., McGrath, M., Burkey, K., Decoteau, D., Fiscus, E., Manning, W., Krupa, S., Chappelka, A., Grantz, D.: The ozone component of global change: potential effects on agricultural an horticultural plant yield, product quality and interactions with invasive species. J. Integr. Plant Biol. **51**, 337–351 (2009)

Bovensmann, H., Burrows, J.P., Buchwitz, M., Frerick, J., Noel, S., Rozanov, V.V., Chance, K.V., Goede, A.P.H.: SCIAMACHY: mission objectives and measurement modes. J. Atmos. Sci. **56**(2), 127–150 (1999)

Bucsela, E.J., Celarier, E.A., Wenig, M.O., Gleason, J.F., Veefkind, J.P., Folkert Boersma, K., Brinksma, E.J.: Algorithm for NO2 vertical column retrieval from the ozone monitoring instrument. IEEE Trans. Geosci. Remote Sens. **44**, (2006). doi:10.1109/TGRS.2005.863715

Burrows, J.P., Weber, M., Buchwitz, M., Rozanov, V., Ladstatter-Weissenmayer, A., Richter, A., DeBeek, R., Hoogen, R., Bramstedt, K., Eichmann, K.U., Eisinger, M.: The global ozone monitoring experiment (GOME): mission concept and first scientific results. J. Atmos Sci. **56**(2), 151–175 (1999)

Byun, D., Schere, K.L.: Review of the governing equations, computational algorithms, and other components of the Models-3 Community Multiscale Air Quality (CMAQ) modeling system. Appl. Mech. Rev. **59**, 51–77 (2006)

Callies, J., Corpaccioli, E., Eisinger, M., Hahne, A., Lefebvre, A.: GOME-2: Metop's second generation sensor for operational ozone monitoring. ESA Bull. **102**, 28–36 (2000)

Carder, K.L., Chen, F.R., Lee, Z.P., Hawes, S.K., Kamykowski, D.: Semianalytic Moderate-Resolution Imaging Spectrometer algorithms for chlorophyll and absorption with bio-optical domains based on nitrate-depletion temperatures. J. Geophys. Res. **104**(C3), 5403–5421 (1999)

Castro, M.S., Driscoll, C.T., Jordan, T.E., Reay, W.G., Boynton, W.R.: Sources of nitrogen to estuaries in the United States. Estuaries **26**(3), 803–814 (2003)

Celarier, E.A., et al.: Validation of ozone monitoring instrument nitrogen dioxide columns. J. Geophys. Res. **113**, D15S15 (2008). doi:10.1029/2007JD008908

Choi, Y. et al.: Evidence of lightning NO_x and convective transport of pollutants in satellite observations over North America. Geophys. Res. Lett. **32** (2005)

Intergovernmental Panel on Climate Change: Climate Change 2007: The Physical Science Basis. Contribution of Working Group I to the Fourth Assessment Report of the Intergovernmental Panel on Climate Change, edited by S. Solomon et al., Cambridge Univ. Press, Cambridge (2007)

Crutzen, P.J.: The role of NO and NO_2 in the chemistry of the troposphere and stratosphere. Ann. Rev. Earth Planet. Sci. **7**, 443–472 (1979)

Crutzen, P.J.: Ozone in the troposphere. In: Singh, H.B. (ed.) Composition, chemistry and climate of the atmosphere, pp. 349–393. Van Nostrand Reinhold, New York (1995)

Daumont, M., Brion, J., Charbonnier, J., Malicet, J.: Ozone UV spectroscopy, I: absorption cross-sections at room temperature. J. Atmos. Chem. **15**, 145–155 (1992)

Dennis R.L.: Model estimated oxidized nitrogen deposition not covered by the networks with a focus on urban deposition, NADP 2007 Scientific Symposium, Boulder (2007)

Environmental Protection Agency: National air quality and emissions trends report 1998, Rep. EPA 454/R-00-003 (1998)

Environmental Protection Agency: Overview of the Human Health and Environmental Effects of Power Generation: Focus on Sulfur Dioxide (SO2), Nitrogen Oxides (NO_x) and Mercury (Hg), (2002) http://www.epa.gov/air/clearskies/pdfs/overview.pdf

Fishman, J., Creilson, J.K., Parker, P.A., Ainsworth, E.A., Vining, G.G., Szarka, J., Booker, F.L., Xu, X.: An investigation of widespread ozone damage to the soybean crop in the upper Midwest determined from ground-based and satellite measurements. Atmos. Environ. **44**, 2248–2256 (2010)

Fishman, J., Iraci, L.T., Al-Saadi, J., Bontempi, P., Chance, K., Chavez, F., Chin, M., Coble, P., Davis, C., DiGiacomo, P., Edwards, D., Eldering, A., Goes, J., Herman, J., Hu, C., Jacob, D., Jordan, C., Kawa, S.R., Key, R., Liu, X., Lohrenz, S., Mannino, A., Natraj, V., Neil, D., Neu, J., Newchurch, M., Pickering, K., Salisbury, J., Sosik, H., Subramaniam, A., Tzortziou, M., Wang, J., Wang, M.: "The United States' Next Generation of Atmospheric Composition and Coastal Ecosystem Measurements: NASA's Geostationary Coastal and Air Pollution Events (GEO APE) Mission". Bull. Am. Meteorol. Soc. (2012)

Gordon, H.R.: Atmospheric correction of ocean color imagery in the Earth Observing System era. J. Geophys. Res. **102**(D14), 17081–17106 (1997)

Grobner, J., Kerr, J.B.: Ground-dased determination of ultraviolet extraterrestrial solar irradiance: providing a link between space-based and ground-based solar UV measurements. J. Geophys. Res. **106**(D7), 7211–7217 (2001)

Gu, B., Zhu, Y., Chang, J., Peng, C., Liu, D., Min, Y., Luo, W., Howarth, R.W., Ge, Y.: The role of technology and policy in mitigating regional nitrogen pollution. Env. Res. Lett. **6**, 014011 (2011). doi:10.1088/1748-9326/6/1/014011

Herman, J.R., Cede, A., Spinei, E., Mount, G., Tzortziou, M., Abuhassan, N.: NO2 column amounts from ground-based Pandora and MFDOAS spectrometers using the direct-sun DOAS technique: intercomparisons and application to OMI validation. JGR-Atmos. **114**, D13307 (2009). doi:10.1029/2009JD011848

Jickells, T.: The role of air-sea exchange in the marine nitrogen cycle. Biogeosci. Discuss. **3**, 183–210 (2006)

Krotkov, N.A., and the OMI NO_2 Algorithm Team: OMNO2 README File, Document Version 6.2 (2012) http://disc.sci.gsfc.nasa.gov/Aura/data-holdings/OMI/documents/v003/OMNO2_readme_v003.pdf

Kurucz, R.L.: New atlases for solar flux, irradiance, central intensity, and limb intensity. Presented at the workshop "ATLAS12 and related codes" held in Trieste 11–15 July, 2005 to be published on Memorie della Societa Astronomica Italiana Supplementi **8**, 158–160 (2005)

Levelt, P.F., van den Oord, G.H.J., Dobber, M.R., Ma¨lkki, A., Visser, H., de Vries, J., Stammes, P., Lundell, J.O.V., Saari, H.: The ozone monitoring instrument. IEEE Trans. Geosci. Remote Sens. **44**(5), 1093–1101 (2006)

Loughner, C.P., Allen, D.J., Pickering, K.E., Dickerson, R.R., Zhang, D.-L., Shou, Y.-X.: Impact of the Chesapeake Bay breeze and fair-weather cumulus clouds on pollutant transport and transformation. Atmos. Environ. **45**, 4060–4072 (2011)

Loughner, C.P., Tzortziou ,M., Follette-Cook, M., Pickering, K.E., Goldberg, D., Satam, C., Weinheimer, A., Crawford, J.H., Knapp, D.J., Montzka, D.D., Diskin, G.B., Marufu, L.T., Dickerson, R.R.:Impact of bay breeze circulations on surface air quality and boundary layer export, submitted to Atmospheric Environment (2013)

Mannino, A., Russ, M.E., Hooker, S.B.: Algorithm development for satellite-derived distributions of DOC and CDOM in the U.S. Middle Atlantic Bight. J. Geophys. Res. **C07051**, (2008). doi:10.1029/2007JC004493

O'Reilly, J.E., Maritorena, S., O'Brien, M.C., Siegel, D.A., Toole, D., Menzies, D., Smith, R.C., Mueller, J.L., Mitchell, B.G., Kahru, M., Chavez, F.P., Strutton, P., Cota, G.F., Hooker, S.B., McClain, C., Carder, K.L., Muller-Karger, F., Harding, L., Magnuson, A., Phinney, D., Moore, G.F., Aiken, J., Arrigo, K.R., Letelier, R., Culver, M.: Ocean color chlorophyll a algorithms for SeaWiFS, OC2, and OC4: Version 4. In: Hooker, S.B., Firestone, E.R. (eds.) SeaWiFS Postlaunch Calibration and Validation Analyses, Part 3 (pp. 9–23). NASA Tech. Memo. 2000-206892, Vol. 11. NASA Goddard Space Flight Center, Greenbelt (2000)

OAQPS Staff Paper: Review of National Ambient Air Quality Standards for Ozone - Assessment of Scientific and Technical Information. Office of Air Quality Planning and Standards, EPA (1996)

Palmer, P.I., Jacob, D.J., Chance, K., Martin, R.V., Spurr, R.J.D., Kurosu, T.P., Bey, I., Yantosca, R., Fiore, A.: Air mass factor formulation for spectroscopic measurements from satellites: application to formaldehyde retrievals from the global ozone monitoring experiment. J. Geophys. Res. **106**, 14539 (2001)

Parrish, D.D., Millet, D.B., Goldstein, A.H.: Increasing ozone concentrations in marine boundary layer air inflow at the west coasts of North America and Europe. Atmos. Chem. Phys. **9**, 1303e1323 (2009)

Pineda Rojas, A.L., Venegas, L.E.: Atmospheric deposition of nitrogen emitted in the Metropolitan Area of Buenos Aires to coastal waters of de la Plata River. Atmos. Environ. **43**, 1339–1348 (2009)

Platt, U.: Differential Optical Absorption Spectroscopy(DOAS), in: air monitoring by Spectroscopic Techniques, edited by: Sigrist, M. W. Chem. Anal. **127**, 27–76 (1994)

Reed A.J., Thompson, A.M., Kollonige, D.E., Martins, D.K., Tzortziou, M.A., Herman, J.R., Berkoff, T.A., Abuhassan, N.K., Cede, A: Effects of Local Meteorology and Aerosols on Ozone and Nitrogen Dioxide Retrievals from OMI and Pandora Spectrometers in Maryland, USA during DISCOVER-AQ 2011. J. Atmos. Chem. (This Issue)

Richter, A., Burrows, J.P., Nüs zlig, H., Granier, C., Niemeier, U.: Increase in tropospheric nitrogen dioxide over China observed from space (and Supplementary Discussion on: error estimates for changes in tropospheric NO2 columns as derived from satellite measurements). Nature **437**, 129–132 (2005)

Sanders, G.E., Colls, J.J., Clark, A.G.: Physiological changes to Phaseolus vulgarisin response to long-term ozone exposure. Ann. Bot. **69**, 123–133 (1992)

Seinfeld, J.H., Pandis, S.N.: Atmospheric chemistry and physics – from air pollution to climate change. John Wiley & Sons, New York (1998)

Skamarock, W.C., Klemp, J.B., Dudhia, J., Gill, D.O., Barker, D.L., Duda, M.G., Huang, X.-Y., Wang, W., Powers, J.G.: A description of the Advanced Research WRF Version 3, NCAR Technical Note, NCAR/TN-475+STR. NCAR, Boulder (2008)

Solomon, S.: Stratospheric ozone depletion: a review of concepts and history. Revs. Geophys. **37**, 275–316 (1999)

STAC Publ. 09-001: Workshop on Atmospheric Deposition of Nitrogen, Chesapeake Bay Program, Science and Technical Advisory Committee, January 8, 2009, Held May 30, 2007 at the State University of New York, Binghamton, NY, Co-Chairs: R. Entringer and R. Howarth (2009)

Tzortziou, M., Herman, J.R., Cede, A., Abuhassan, N.: High precision, absolute total column ozone measurements from the Pandora spectrometer system: comparisons with data from a Brewer double monochromator and Aura OMI. J. Geophys. Res. **117**, D16303 (2012). doi:10.1029/2012JD017814

Van Hoosier, M.E.: The ATLAS-3 solar spectrum, available via anonymous ftp (1996) (ftp://susim.nrl.navy.mil/pub/atlas3)

Vandaele, A.C., Hermans, C., Simon, P.C., Carleer, M., Colin, R., Fally, S., Mérienne, M.F., Jenouvrier, A., Coquart, B.: Measurements of the NO_2 absorption cross-section from 42 000 cm–1 to 10 000 cm–1 (238–1,000 nm) at 220 K and 294 K. J. Quant. Spectrosc. Radiat. Transfer **59**(3–5), 171–184 (1998)

Velders, G.J.M., Grainer, C., Portmann, R.W., Pfeilsticker, K., Weing, M., Wagner, T., Platt, U., Richter, A., and Burrows, J.P.: Global tropospheric NO_2 column distributions: Comparing three-dimensional model calculations with GOME measurements, J. Geophys. Res. **106**(D12) (2001)

Vingarzan, R.: A review of surface ozone background levels and trends. Atmos. Environ. **38**, 3431e–3442e (2004)

Wang, S., Pongetti, T.J., Sander, S.P., Spinei, E., Mount, G.H., Cede, A., Herman, J.: Direct Sun measurements of NO2 column abundances from Table Mountain, California: Intercomparison of low- and high-resolution spectrometers. J. Geophys. Res. **115**, D13305 (2010). doi:10.1029/2009JD013503

Wenig, M., Spichtinger, N., Stohl, A., Held, G., Beirle, S., Wagner, T., Jahne, B., Platt, U.: Intercontinental transport of nitrogen oxide pollution plumes. Atmos. Chem. Phys. **3**, 387–393 (2003)